Solution Structure of a Polypeptide from the N Terminus of the HIV Protein Nef

Kevin J. Barnham, Stephen A. Monks, Mark G. Hinds, Ahmed A. Azad, and Raymond S. Norton*

Biomolecular Research Institute, 343 Royal Parade, Parkville, Victoria 3052, Australia

Received December 6, 1996; Revised Manuscript Received March 10, 1997[⊗]

ABSTRACT: Nef is a 27 kDa myristylated phosphoprotein expressed early in infection by HIV. The N terminus of Nef is thought to play a vital role in the functions of this protein through its interactions with membrane structures. The solution structure of a 25-residue polypeptide corresponding to the N terminus of Nef (Nef1−25) has been investigated by ^{1}H NMR spectroscopy. In aqueous solution at pH 4.8 and 281 K, this peptide underwent conformational averaging, with Pro13 existing in *cis* and *trans* conformations in nearly equal proportions. In methanol solution, however, the peptide adopted a well-defined α-helical structure from residues 6 to 22, with the N- and C-terminal regions having a less ordered structure. On the basis of a comparison of chemical shifts and NOEs, it appeared that this helical structure was maintained in aqueous trifluoroethanol (50% v/v) and to a lesser extent in a solution of SDS micelles. When the *N*-acetyl group was replaced by either an *N*-myristyl or a free ammonium group, there was little effect on the three-dimensional structure of the peptide in methanol; deamidation of the C terminus also had no effect on the structure in methanol. In water, the myristylated peptide aggregated. The similarity between the sequences of Nef1−25 and melittin is reflected in the similar structures of the two molecules, although the N-terminal helix of melittin is more defined. This similarity in structure raises the possibility that Nef1−25 not only interacts with membranes but also may be capable of disrupting them and causing cell lysis. This type of interaction could contribute at least in part to the killing of bystander cells in lymphoid tissues during HIV infection.

The human immunodeficiency virus (HIV)[1] produces a range of accessory proteins which are not required for virus replication *in vitro* but appear to be essential *in vivo* for virus infection and pathogenicity (Trono, 1995). One of these is Nef (negative factor), a 27 kDa myristylated phoshoprotein associated with cytoplasmic membrane structures in HIV-infected cells (Allan et al., 1985; Guy et al., 1987). While the exact function of Nef remains controversial, there appears to be little doubt that Nef plays an important role in the progression of the disease to acquired immunodeficiency syndrome (AIDS). Consistent deletions within the Nef gene have been found in long-term HIV-infected patients who have not progressed to AIDS (Deacon et al., 1995). Similar results have been found in monkeys infected with the related simian immunodeficiency virus, where virus which lacked the Nef gene replicated poorly and little progression of the disease was observed (Kestler et al., 1991). Nef is expressed early in HIV infection and at particularly high levels (Cullen, 1994); its effects include induction of CD4 down-regulation, alteration of T cell activation pathways, and enhancement of virus infectivity (Trono, 1995).

Recently, Grzesiek et al. (1996) determined the solution structure of a Nef construct with significant deletions at the N terminus (residues 2−39) and near the C terminus (residues 159−173). It was stated that the deleted residues were unstructured and, in the case of the N-terminal residues, were also responsible for aggregation of the protein. The 2−39 and 159−173 deletions appeared not to affect the interaction between Nef and the SH3 domain of Hck tyrosine kinase, which is dependent on a PXX repeat segment in the core of Nef (residues 69−78) and may play a role in the promotion of virus replication (Saksela et al., 1995; Schwartz et al., 1995). Subsequently, the X-ray crystal structure of residues 54−205 of Nef in complex with a mutant of the Fyn SH3 domain has also been described and is in good agreement with the NMR structure (Lee et al., 1996).

While the N terminus of Nef apparently had no effect on the interaction between Nef and SH3 domains, there is evidence that it plays a key role in other functions of the protein (Goldsmith et al., 1995). Analysis of Nef gene sequences from virus subtype B showed that residues 2−7 and 20 were highly conserved, whereas residues 8−15 were poorly conserved with the exception of Gly12 and Trp13, which are also conserved (Shugars et al., 1993). A similar study by Artenstein et al. (1996) on subtype E of HIV found that residues 1−30 were more highly conserved than reported by Shugars et al. Both groups referred to the highly conserved region of residues 2−7 as the myristylation signal. However, for other myristylated retroviral proteins such as Gag, only Gly2 is required as a myristylation signal and considerable sequence diversity can be tolerated in the following residues (Kaplan et al., 1988). The highly conserved nature of these residues in Nef therefore suggests that they may have some other function. This was confirmed by Goldsmith et al. (1995), who showed that deletion of

* To whom correspondence should be addressed. Fax: +61 3 9903 9655. E-mail: ray@mel.dbe.csiro.au.

[⊗] Abstract published in *Advance ACS Abstracts,* May 1, 1997.

[1] Abbreviations: HIV, human immunodeficiency virus; Nef, negative factor; AIDS, acquired immunodeficiency syndrome; TFE, 2,2,2-trifluoroethanol; MeOH, methanol; SDS-$^2H_{25}$, deuterated sodium dodecyl sulfate; NMR, nuclear magnetic resonance; 1D, one-dimensional; 2D, two-dimensional; NOE, nuclear Overhauser enhancement; NOESY, nuclear Overhauser enhancement spectroscopy; DQF-COSY, double-quantum-filtered scalar-correlated spectroscopy; TOCSY, total correlation spectroscopy; E-COSY, exclusive correlation spectroscopy; HMQC, heteronuclear multiple-quantum coherence; rms, root mean square; CSI, chemical shift index.

S0006-2960(96)02994-7 CCC: $14.00

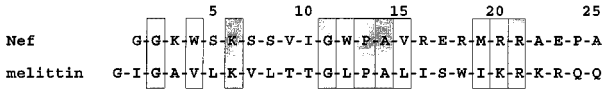

FIGURE 1: Comparison of the sequences of the 25-residue polypeptide from the N terminus of Nef (Nef1−25) and bee venom melittin. Identical residues are shown in shaded boxes, while the analogous residues are in open boxes.

residues 4−7 of Nef resulted in a "dramatically impaired enhancement of infectivity". The mutant also had a significantly reduced ability to down-regulate CD4, although a highly conserved glutamic acid-rich region (residues 60−71) of the protein was also identified as being crucial to this activity of Nef.

A similar result was obtained by Greenway et al. (1994), who showed that Nef caused down-regulation of the surface expression of CD4 and IL2-R when electroporated into T-lymphocytes, but this did not occur with Nef lacking the 19 N-terminal residues. When peripheral blood mononucleocytes were treated with Nef, the intracellular targets of Nef included CD4, p53, p44$^{mapk/erk1}$, and p56^{lck}, whereas Nef with the first 19 residues deleted had only a weak interaction with p56^{lck} (Greenway et al., 1995). In addition, cells treated with full-length Nef showed a reduced proliferative response to exogenous recombinant IL-2, as well as inhibition of p56^{lck} activity and post-translational modification, while the truncated Nef had no significant effect. Thus, the N terminus of Nef could be involved, either directly or indirectly, in interactions with cellular proteins involved in intracellular signaling and apoptosis and in inhibition of their activities. Macreadie et al. (1995) showed that both the N terminus and the myristyl group of Nef were important in the release into culture medium of Nef from *Saccharomyces cerevisiae* cells subjected to stress, suggesting that the N terminus may also be important in membrane targeting.

The basis for at least one possible function of the N terminus was indicated by Curtain et al. (1994), who showed that full-length, nonmyristylated Nef had membrane-perturbing capabilities, as shown by its ability to fuse small unilamellar dipalmitoylphosphatidylcholine vesicles and induce the formation of nonlamellar lipid structures. Importantly, Nef with the first 18 residues deleted had no such effects, whereas a peptide consisting of the first 18 residues of Nef did. A similarity was also noted between the sequences of the N terminus of Nef and bee venom melittin, which is a membrane-active peptide (Figure 1). The first 21 residues of Nef have six conserved and five conservatively substituted residues compared with melittin, and both peptides have a centrally located proline, at position 13 and 14 in Nef1−25 and melittin, respectively.

The importance of the N terminus of Nef to its function, as well as its sequence similarity to melittin, led us to investigate the solution structure of the polypeptide Nef1−25, corresponding to the first 25 residues of human Nef. Nef1−25 was N-terminally acetylated and C-terminally amidated. We report here the complete NMR resonance assignments and structure in methanol of Nef1−25. Studies of melittin (Bazzo et al., 1988; Brown & Wüthrich, 1981; Brown et al., 1982; Inagaki et al., 1989; Ikura et al., 1991) and δ-hemolysin (Lee et al., 1987; Tappin et al., 1988) have shown that the structures of these molecules in methanol are very similar to their structures in micelles. As micelles are often used to study molecules in lipid environments, these results suggest that methanol is also a suitable solvent for mimicking the structures of peptides associated with lipid membranes. We have also characterized the conformation of the Nef1−25 in aqueous and aqueous/2,2,2-trifluoroethanol (TFE) solutions and investigated the effects of altering the N- and C-terminal groups. The results are discussed in relation to the function of this region of Nef.

MATERIALS AND METHODS

Materials. Peptides were synthesized using the FastMoc method. The myristyl group was added to the peptide using the same method as used for tyrosine (this protocol was chosen because tyrosine requires a longer reaction time than most other amino acids). The crude peptides were purified by reversed phase high-performance liquid chromatography on a Waters HPLC system using a Vydac C18 reverse phase column. Deuterated solvents were obtained from Cambridge Isotope Laboratories (Woburn, MA). Deuterated sodium dodecyl sulfate (SDS-$^2H_{25}$) was supplied by MSD Isotopes.

NMR Spectroscopy. NMR samples were prepared by dissolving the lyophilized Nef1−25 peptides in 0.55 mL of the appropriate solvent (final concentration of 1.5 mM); solvents used were C^2H_3OH, $C^2H_3O^2H$, 90% H_2O/10% ^2H_2O, and ^2H_2O. The pH was adjusted with small additions of 0.5 M NaO^2H or ^2HCl. Nef1−25 was also examined in SDS micelles; a 400 mM solution of SDS-$^2H_{25}$ was prepared in 1 mL of 90% H_2O/10% ^2H_2O, and then 2.4 mg of Nef1−25 was dissolved in 0.6 mL of this solution and the pH adjusted to 5.1. Reported pH values were recorded at room temperature and were not corrected for isotope or solvent effects. The ^1H chemical shifts were referenced to 2,2-dimethyl-2-silapentane-5-sulfonate (DSS) at 0 ppm, via the chemical shift of residual CH_3OH at a δ_{CH_3} of 3.35 ppm (Wüthrich, 1976) or the H_2O resonance (Wishart et al., 1995a).

Spectra were recorded on Bruker AMX-500 or AMX-600 spectrometers. Most spectra were recorded at 281 K, with probe temperatures calibrated according to the method of van Geet (1970). NMR spectra of SDS solutions were recorded at 298 K; attempts to accumulate spectra at lower temperatures resulted in the crystallization of SDS from solution. All 2D spectra were recorded in the phase-sensitive mode using time-proportional phase incrementation (Marion & Wüthrich, 1983). Solvent suppression was achieved by selective, low-power irradiation of the water signal during the relaxation delay (typically 2 s) and during the mixing time in NOESY experiments. For some spectra obtained in 90% H_2O/10% ^2H_2O, water suppression was also achieved by pulsed field gradients using the WATERGATE method of Piotto et al. (1992).

2D homonuclear NOESY spectra (Anil-Kumar et al., 1980; Macura et al., 1981) were recorded with mixing times of 50 and 300 ms. TOCSY spectra (Braunschweiler & Ernst, 1983) were recorded using the DIPSI-2 spin-lock sequence (Rucker & Shaka, 1989) with spin-lock times of 70−80 ms. DQF-COSY (Rance et al., 1983) and E-COSY (Griesinger et al., 1987) spectra were also recorded. Typically, spectra were acquired with 400−600 t_1 increments, 32−128 scans per increment, 4096 data points, and ^1H sweep widths of 6024.1 Hz at 500 MHz and 7812.5 Hz at 600 MHz. Spectra were processed using UXNMR, version 941001.4 (Bruker), and analyzed using XEASY, version 1.3.7 (Bartels et al.,

1995). Sine-squared window functions, phase shifted by 60−90°, were applied in both dimensions prior to Fourier transformation. A ^{13}C HMQC spectrum (Bax et al., 1983) was acquired on Nef1−25 (1.5 mM) dissolved in $C^2H_3O^2H$ (pH 4.8, 281 K) at 600 MHz. The ^{13}C sweep width was 11 318 Hz, and 256 scans and 400 t_1 increments were employed.

The $^3J_{NHC^\alpha H}$ coupling constants were measured from the DQF-COSY spectrum at 500 MHz. The appropriate rows were extracted from the spectrum, inverse Fourier transformed, zero-filled to 32K, and multiplied by a Gaussian window function prior to Fourier transformation. The antiphase peak shapes were simulated to take account of the effect of broad line widths on small coupling constants, using an in-house program COUPLING. Slowly exchanging amide protons were identified by dissolving the lyophilized peptide in the appropriate deuterated solvent ($C^2H_3O^2H$ or ^2H_2O) and recording a series of 1D and TOCSY spectra immediately after dissolution; each TOCSY spectrum had an accumulation time of 7 h, and spectra were recorded for 48 h.

Structural Constraints. NOESY cross-peak volumes measured from a 300 ms mixing time spectrum in C^2H_3OH were used to calculate upper bound distance restraints. Peaks from the upper side of the diagonal were used except where peaks from the lower side were better resolved. Only one pair of nondegenerate $C^\beta H$ protons (Pro13) was free of spectral overlap. As a result, volumes were calibrated using C(6)H−C(7)H cross-peaks from the Trp4 and Trp12 aromatic rings (distance of 2.47 Å); distances were calculated using volumes proportional to r^{-6} in the program CALIBA (Güntert et al., 1991), which automatically corrects for degenerate atoms and pseudoatoms. Where cross-peak volume could not be estimated reliably, an upper bound of 5 Å was assigned. Corrections of 0.5 and 1.0 Å were added to distance constraints involving only backbone protons and at least one side chain proton, respectively, to allow for conformational averaging and errors in volume integration.

A small number of lower bound restraints of >1.8 Å (Wilcox et al., 1993; Manoleras & Norton, 1994) was also used for NH, $C^\alpha H$, and $C^\beta H$ atoms in the final structure calculations. These were obtained with an in-house program which checked the initial (DIANA) structures for distances of <3.5 Å that were not represented in the NOE restraint list. Distances identified in this way were compared with the experimental NOESY spectra to confirm that cross-peaks could have been observed had they been present. Where a cross-peak was clearly absent, a lower bound restraint of 3.5 Å was added to the restraint list; for all other NH, $C^\alpha H$, and $C^\beta H$ atoms, the lower limit was 1.79 Å.

Backbone dihedral angle constraints were inferred from $^3J_{NHC^\alpha H}$ values as follows: $^3J_{NHC^\alpha H} \leq 5$ Hz, $\phi = -60 \pm 30°$; 5 Hz $< {}^3J_{NHC^\alpha H} <$ 6 Hz, $\phi = -60 \pm 40°$; $^3J_{NHC^\alpha H} \geq 8$ Hz, $\phi = -120 \pm 40°$ (Wüthrich, 1986). Where 6 Hz $< {}^3J_{NHC^\alpha H} <$ 8 Hz, and the possibility of positive ϕ angles had been excluded by the NOESY spectrum (Ludvigsen & Poulsen, 1992), ϕ was constrained to $-120 \pm 60°$; otherwise, ϕ angles were not constrained. Nondegenerate $C^\beta H$ resonances were observed for 11 residues at pH 4.5 and 281 K in C^2H_3OH. Where possible, $^3J_{C^\alpha HC^\beta H}$ coupling constants were measured from passive couplings as displacements in E-COSY spectra or peak splittings in DQF-COSY spectra. The relative intensities of intraresidue $d_{\alpha\beta}$ and $d_{N\beta}$ NOEs were measured in a 50 ms mixing time NOESY spectrum. None of the patterns fitted those expected for any of the three staggered conformations ($\chi^1 = -60$, 60, or 180°) (Wagner et al., 1987), as a result of which all χ^1 angles were left unconstrained.

Structure Calculations. Initial structures were generated with the distance geometry program DIANA, version 2.8 (Güntert et al., 1991), using dihedral angle constraints derived from coupling constant data and distance constraints derived from NOE cross-peaks assigned unambiguously in both chemical shift dimensions. No hydrogen bonding restraints were used at any stage in the calculations. Ambiguous NOESY cross-peak assignments were resolved where possible using these initial structures, with an assignment being accepted if in all structures the appropriate interproton distance was <5 Å and the distance between alternative pairs was >7 Å. A small number of lower bound restraints of >1.8 Å was also introduced prior to the final structure calculations.

Once the final set of restraints had been obtained, a new family of distance geometry structures was generated using DIANA, and the 100 structures with the lowest penalty functions were refined by simulated annealing in X-PLOR, version 3.1 (Brünger, 1992). Simulated annealing was performed using 20 000 steps at 1000 K and 10 000 steps as the molecule was gradually cooled to 300 K. A time step of 1 fs was employed throughout. The 100 structures were then subjected to further simulated annealing, in which they were gradually cooled from 300 to 0 K in 20 000 steps and then energy-minimized using 100 steps of Powell conjugate gradient minimization. For each structure, this procedure was carried out 10 times, and the best of these 10 in terms of total energy and NOE energies was selected. The structures were then energy-minimized in the empirical CHARMm force field (Brooks et al., 1983), with all explicit charges neutralized (Monks et al., 1995) and with a distance-dependent dielectric instead of explicit water molecules. The 20 structures that were the best on the basis of their stereochemical energies (i.e. the sum of all contributions to the calculated energy except the electrostatic term) and NOE energies were chosen for structural analysis. This family of 20 structures, together with the NMR retraints used in their determination, have been deposited with the Brookhaven Protein Data Bank (accession number 1ZEC) (Bernstein et al., 1977).

RESULTS

Nef1−25 in Aqueous Solution. 1D and 2D ^1H NMR spectra of Nef1−25 in 90% H_2O/10% ^2H_2O and ^2H_2O at pH 4.8 and 281 K indicated that the peptide had no well-defined structure in aqueous solution. This was evident from the limited dispersion of the backbone NH ($\Delta\delta = 0.6$ ppm) and $C^\alpha H$ ($\Delta\delta = 0.9$ ppm) chemical shifts and the lack of cross-peaks other than intraresidue and sequential cross-peaks in the NOESY spectrum. When the peptide was dissolved in ^2H_2O, the amide protons underwent rapid deuteration (complete within 10 min at 281 K and pH 4.8), indicating an absence of stable hydrogen bonds.

In aqueous solution, the peptide bond preceding Pro13 coexisted in both *cis* and *trans* conformations. The conformation of the Trp−Pro peptide bond, as determined from sequential NOEs between the Trp12 $C^\alpha H$ and the Pro $C^\delta H$ (*trans* conformation) or $C^\alpha H$ (*cis* conformation) resonances (Wüthrich, 1986), was approximately 55% *trans* and 45%

cis, and the interconversion rate between the two forms was sufficiently slow for observation of separate sets of peaks for a number of residues. Only one set of signals was observed for residues 1−6, indicating that any conformational differences associated with *cis*−*trans* isomerism at Pro13 had negligible effects on the chemical shifts of these residues. From Ser7 to Ala25, two sets of signals were observed for most residues, and it was possible to follow the sequential assignment of the two forms from Ser7 to Glu17, although spectral overlap prevented the assignment of peaks from Arg18 to Ala25 to individual conformers. For some residues, the chemical shift difference between the two conformations was >0.1 ppm. The largest difference was for Pro13 $C^{\alpha}H$, which resonated at 3.30 ppm in the *cis* configuration, 1.12 ppm upfield of its random coil value (Wishart et al., 1995b) and 0.93 ppm upfield of the corresponding shift in the *trans* conformer. This large shift to higher field may have been the result of ring-current effects (Wüthrich, 1986) from the neighboring Trp12.

Only three medium-range NOE cross-peaks were observed in the NOESY spectrum of Nef1−25 in aqueous solution, as follows: Ile10, $d_{NN}(i,i+2)$; Trp12, $d_{\alpha N}(i,i+2)$ and $d_{NN}(i,i+2)$. These cross-peaks were all associated with the conformer having Pro13 in the *cis* configuration, suggesting that this conformer may have a slightly more stable structure than the *trans* conformer.

Cis−*trans* isomerism was also observed for Pro24, but only a small proportion (<5%) was present in the *cis* form. The presence of the *cis* isomer was confirmed by observation of a weak NOESY cross-peak from Glu23 $C^{\alpha}H$ to Pro24 $C^{\alpha}H$. Only the flanking residues Glu23 and Ala25 gave rise to separate NMR cross-peaks due to this conformation, indicating that the structural differences between the two forms were limited, in contrast to those due to Pro13 isomerism.

TFE has been used extensively to stabilize helical structures in aqueous solutions (Nelson & Kallenbach, 1986; Dyson et al., 1992; Sönnichsen et al., 1992; Morton et al., 1994). When trifluoroethanol (TFE) was titrated (up to 50%) into an aqueous solution of Nef1−25 (the pH increased from 4.8 to 5.5), there was a small increase in the dispersion of the backbone NH chemical shifts (to 0.7 ppm) and a larger increase (to 1.4 ppm) in the $C^{\alpha}H$ chemical shift dispersion. The effect of *cis*−*trans* isomerism at Pro13 became less pronounced at a TFE concentration around 30% and disappeared once the TFE concentration reached 50%. Not only did the $C^{\alpha}H$ resonances have a greater chemical shift dispersion in 50% TFE, but several also shifted to higher field (Figure 2A), consistent with formation of a helical structure. In fact, the profile of the $C^{\alpha}H$ chemical shift index is very similar to that of Nef1−25 in methanol (Figure 2B), the structure of which is discussed below. These results are in broad agreement with those of Sabatier et al. (1990), who found using circular dichroism spectroscopy that a peptide corresponding to residues 1−31 of Nef was partially helical in TFE but a mixture of β-sheet and random structures in aqueous solution, whereas a shorter peptide (residues 1−17) was not helical in either solvent and actually formed a β-sheet in TFE.

The polypeptides melittin (Bazzo et al., 1988; Brown & Wüthrich, 1981; Brown et al., 1982; Inagaki et al., 1989; Ikura et al., 1991) and δ-hemolysin (Lee et al., 1987; Tappin et al., 1988) have very similar structures in methanol and lipid micelles, implying that methanol is an appropriate solvent for mimicking structures of peptides in membrane-like environments. When Nef1−25 was dissolved in methanol, 1D and 2D spectra were consistent with an α-helical structure (the $C^{\alpha}H$ $\Delta\delta$ is shown in Figure 2B) and there was a good correlation between spectra in methanol and those in 50% H_2O/TFE (i.e. similar chemical shifts and NOESY cross-peaks). As the overall quality of the spectra recorded in methanol was superior to the quality of those in 50% H_2O/TFE (better signal-to-noise and resolution), the methanol spectra were used to calculate the structure of Nef1−25.

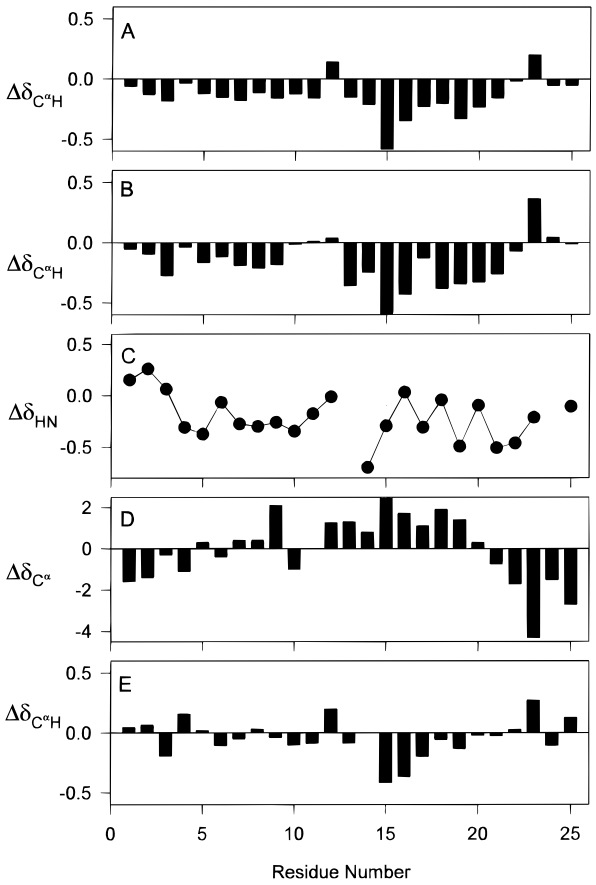

FIGURE 2: Chemical shift analyses for Nef1−25. All random coil chemical shifts are taken from Wishart et al. (1995b). (A) Deviation of the $C^{\alpha}H$ chemical shift from random coil values for Nef1−25 in 50% H_2O/50% TFE at pH 5.5 and 281 K. (B) Deviation of the $C^{\alpha}H$ chemical shift from random coil values for Nef1−25 in C^2H_3OH at pH 4.5 and 281 K. (C) Deviation of the NH chemical shift from random coil values for Nef1−25 in C^2H_3OH at pH 4.5 and 281 K. (D) Deviation of the C^{α} chemical shift from random coil values for Nef1−25 in $C^2H_3O^2H$ at pH 4.8 and 281 K. (E) Deviation of the $C^{\alpha}H$ chemical shift from random coil values for Nef1−25 in SDS micelles at pH 5.1 and 298 K.

Nef1−25 Assignments in Methanol. Spin systems of the peptide dissolved in C^2H_3OH were assigned using a combination of DQF-COSY and TOCSY spectra at 281 K, while sequence-specific assignments were made using NOESY spectra (Wüthrich, 1986). Figure 3 shows the fingerprint (Figure 3A) and d_{NN} regions (Figure 3B) of the NOESY spectrum, and the assignments are tabulated in the Supporting Information.

The deviations of $C^{\alpha}H$ and backbone NH from random coil values (Wishart et al., 1995b) are shown in Figure 2. The upfield shifts of the α-protons were compatible with a helical structure, and the gradual upfield shift of the NH

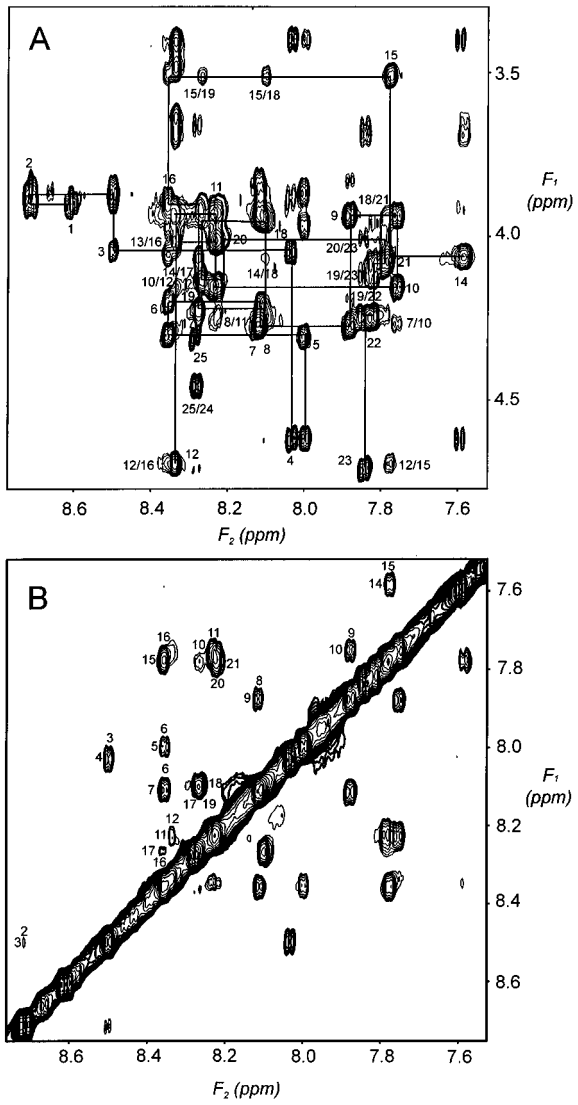

FIGURE 3: Regions of the 300 ms mixing time NOESY spectrum of Nef1−25 in C^2H_3OH at pH 4.5 and 281 K. (A) $C^\alpha H-NH$ region. Intraresidue $NH-C^\alpha H$ cross-peaks are labeled with a single number. Sequential NOE cross-peaks are not labeled but are indicated by the line joining cross-peaks due to consecutive residues (the $C^\alpha H$ chemical shifts of Ala14 and Pro13 are quite close; as a result, the αN connectivity between Pro13 and Ala14 overlapped with the $NH-C^\alpha H$ cross-peak of Ala14). Medium-range cross-peaks are indicated by two numbers indicating the residues contributing the $C^\alpha H$ and NH protons, respectively. (B) NH−NH region. The NH−NH cross-peaks are labeled with two numbers identifying the sequence position of the interacting residues; numbers beside the cross-peak identify the contributing residue from the F_1 dimension, while the numbers above or below the cross-peak identify the contributing residue from the F_2 dimension.

resonances when going from the N to C terminus was consistent with the shielding effect of a helical macrodipole (Wishart et al., 1991). The variation in the NH chemical shift from random coil values (Figure 2C) for residues 6−23 was consistent with a 3−4 repeat pattern observed for α-helices (Zhou et al., 1992), and the C^α chemical shifts shown in Figure 2D were consistent with a helical conformation for residues 12−20. Increasing the temperature from 281 to 298 K had no significant effect on the spectra (the chemical shift range for the $C^\alpha H$ resonances of residues 6−22 decreased only slightly, from 1.20 ppm at 281 K to 1.17 ppm at 298 K), implying that the helical structure was retained over this temperature range.

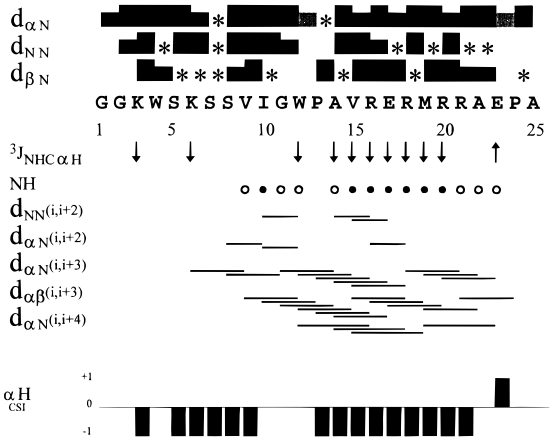

FIGURE 4: Summary of NMR data for Nef1−25 in C^2H_3OH at pH 4.5 and 281 K. The intensities of $d_{\alpha N}$, d_{NN}, and $d_{\beta N}$ connectivities are represented as strong, medium, or weak by the height of the bars. Shaded lines indicate $d_{\alpha\delta}$ connectivities to Pro residues. Asterisks indicate that the presence of a NOE could not be confirmed unambiguously due to peak overlap. Values for $^3J_{HNC^\alpha H}$ of <6 Hz are indicated by ↓, while those of >8 Hz are indicated by ↑. Those left blank could not be measured due to overlap or were between 6 and 8 Hz. The relative exchange rates of backbone NH protons are indicated in the row labeled NH and are based on the strength of cross-peaks in exchange TOCSY experiments; slowly exchanging amides are indicated by filled circles, while open circles indicate intermediate exchange. The row labeled αH shows the chemical shift index of the $C^\alpha H$. If the $C^\alpha H$ deviation from random coil is >0.1 ppm to higher field than the random coil value (Wishart et al., 1995b), it is given a value of −1; if the $C^\alpha H$ value is >0.1 ppm to lower field than the random coil value (Wishart et al., 1995b), it is given a value of 1.

Amide Exchange. When Nef1−25 was dissolved in $C^2H_3O^2H$ at pH 4.5 and 281 K, the amides of residues near the N and C termini exchanged more rapidly, with the NH signals of Gly2, Lys3, Lys6, Ser7, Ser8, Ala25, and the C-terminal amide disappearing within 3 h and those from Gly1, Trp4, and Ser5 disappearing shortly thereafter. The other amides were still present after 24 h, and those from Ile10, Val15, Arg16, Glu17, Arg18, Met19, and Arg20 were observable in a TOCSY spectrum after 48 h (Figure 4). These slowly exchanging amide protons were from the center of the helix, while the amides with intermediate exchange rates (Val9, Arg21, Ala22, and Glu23) were from the ends of the helix. The amides of Gly11, Trp12, and Ala14, although near the center of the helix, were not among the most slowly exchanging group, presumably because of their proximity to Pro13, which is the site of a kink in the helix (see below).

Structure Determination of Nef1−25 in Methanol. Figure 4 summarizes the sequential and medium-range NOE connectivities, $^3J_{NHC^\alpha H}$ coupling constants, and slowly exchanging amide protons observed in methanol. The presence of helical structure encompassing residues 6−22 is indicated by the low $^3J_{NHC^\alpha H}$ coupling constants (<6 Hz), numerous $d_{\alpha N}(i,i+3)$, $d_{\alpha N}(i,i+4)$, and $d_{\alpha\beta}(i,i+3)$ NOE connectivities, and the presence of slowly exchanging backbone amide protons in this region of the molecule. The low coupling constants indicate that under these conditions residues 6−22 were not undergoing significant conformational averaging.

Structures were calculated using 394 upper bound distance constraints inferred from NOEs, made up of 239 intraresidue, 81 sequential, and 73 medium-range ($1 < |i - j| < 5$) NOEs (Figure 5A); only one long-range NOE was observed, between C(4)H of Trp12 and NH of Glu17. Six lower bound

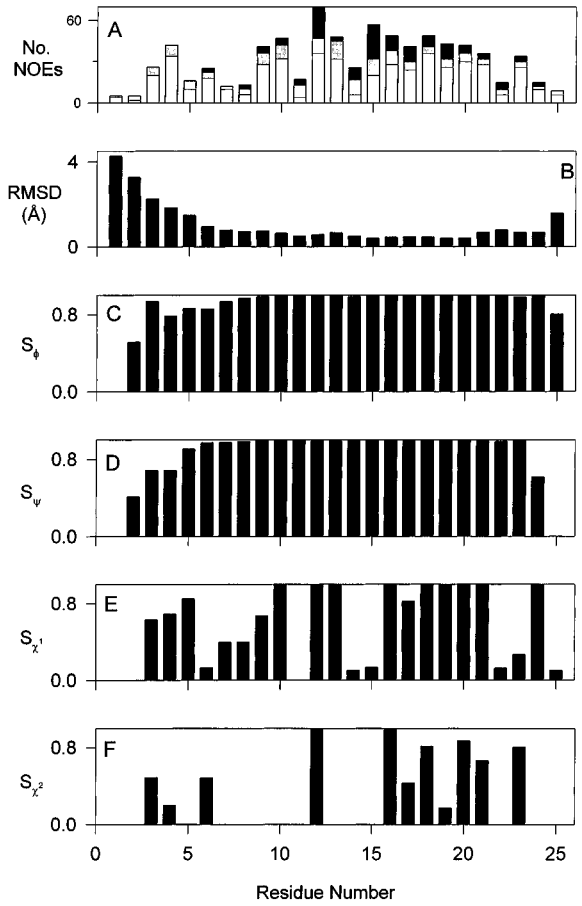

FIGURE 5: Parameters characterizing the final 20 structures of Nef1−25 in methanol, plotted as a function of residue number. (A) Upper bound distance restraints used in the final round of structure refinement. Medium-range ($1 < i - j < 5$), sequential, and intraresidue NOEs are shown in black, hatched, and white shading respectively; the one long-range NOE [Trp12 C(4)H to Glu17 NH] is not shown. NOEs are counted twice, once for each proton involved. (B) rms deviations from the mean structure for the backbone heavy atoms (N, C^α, and C) following superposition over the whole molecule. (C−F) Angular order parameters (S) (Hyberts et al., 1992; Pallaghy et al., 1993) for the backbone (ϕ and ψ) and side chain (χ^1 and χ^2) dihedral angles. Gaps in the χ^1 plot are due to Gly and Ala residues. Gaps in the χ^2 plot, in addition to Gly and Ala, are due to Ser, Pro, and Val residues.

constraints based on the absence of NOEs from the NOESY spectrum were also used. Fourteen backbone dihedral angle constraints based on spin−spin coupling constants were used, but no side chain restraints were employed. Initial structures were calculated using DIANA, then refined by simulated annealing in X-PLOR, and finally energy-minimized in X-PLOR with the CHARMm force field. A summary of geometric and energetic parameters for these structures is given in Table 1.

Structural Analysis and Description. Analysis of the angular order parameters (S) (Hyberts et al., 1992; Pallaghy et al., 1993) of the final 20 structures indicates that residues 7−23 are well-defined, with an S of >0.9 for both ϕ and ψ angles (Figure 5C,D). The rmsd from the mean structure is plotted as a function of residue number in Figure 5B, which shows that the structure is well-defined over the central part of the molecule. For this well-defined region, the mean pairwise rmsd is 0.44 ± 0.14 Å for the backbone heavy atoms C, C^α, and N and 1.51 ± 0.19 Å for all heavy atoms. Corresponding values for the whole molecule are 1.90 ± 0.63 and 2.67 ± 0.64 Å, respectively. Although no χ angles

Table 1: Structural Statistics for the 20 Energy-Minimized Structures of Nef1−25 in Methanol from X-PLOR[a]

rms deviations from experimental distance restraints (Å) (394)[b]	0.0278 ± 0.0009
rms deviations from experimental dihedral restraints (deg) (14)[b]	0.283 ± 0.162
rms deviations from idealized geometry	
bonds (Å)	0.0094 ± 0.0004
angles (deg)	2.442 ± 0.064
impropers (deg)	0.252 ± 0.020
energies (kcal mol^{-1})	
E_{NOE}	9.00 ± 0.82
E_{cdih}	0.08 ± 0.06
E_{L-J}	−80.9 ± 2.6
$E_{bond} + E_{angle} + E_{improper}$	66.3 ± 3.5
E_{elec}	−314.4 ± 10.4

[a] The best 20 structures after energy minimization in the distance geometry force field were subsequently energy-minimized in the CHARMm force field, using a distance-dependent dielectric and neutralized side chains, as described in Materials and Methods. [b] The numbers of restraints are shown in parentheses. None of the structures had distance violations of >0.3 Å or dihedral angle violations of >5°.

were restrained, several of the residues have well-defined χ^1 angles, and some also have well-defined χ^2 angles (Figure 5E,F). These residues with well-defined χ^1 and χ^2 angles are located in the helical region of the molecule.

The overall conformation of Nef1−25 in methanol is shown in Figure 6A, where the backbone heavy atoms and the well-defined side chains of the 20 best structures (those with the lowest overall energies, excluding the electrostatic term) have been superimposed over residues 7−23 (where the molecule is α-helical). An orthogonal view of the structures is presented in Figure 6B.

Structure in Detergent Micelles. The structure of Nef1−25 in methanol has been described in detail because the good quality of the spectra in this solvent permitted an extensive set of NMR restraints to be obtained. We have also investigated the structure in micelles of the detergent SDS. The *cis*−*trans* isomerism about the Trp12−Pro13 amide bond, which was evident in aqueous solution, was not present in SDS micelles, and it is assumed that the *trans* conformer is now dominant, although this could not be confirmed from NOEs to the $C^\alpha H$ resonance of Trp12 as this peak was coincident with the water resonance.

The deviations of $C^\alpha H$ chemical shifts from random coil (Wishart et al., 1995b) (Figure 2E) indicated that residues 13−22 were predominantly α-helical, and several $d_{NN}(i,i+2)$ and $d_{\alpha N}(i,i+3)$ NOESY cross-peaks associated with these residues supported this. While there was no evidence that the first 10 residues were also helical, the observation of several medium-range NOEs, including $d_{NN}(i,i+2)$ for residues 7 and 9 and 8 and 10, $d_{\alpha N}(i,i+2)$ for residues 2 and 4 and 5 and 7, and $d_{\alpha N}(i,i+4)$ for residues 1 and 5, suggested that the N-terminal end of Nef1−25 may be more structured in SDS micelles than in aqueous solution.

Altered N and C Termini. The effects of replacing the *N*-acetyl group of Nef1−25 with a myristyl group were examined in C^2H_3OH at 281 K and pH 4.5. Only small changes were observed in the chemical shifts of the three N-terminal residues compared with those of Nef1−25, the largest difference in NH and $C^\alpha H$ chemical shifts being observed for Gly1 ($\delta_{NH} = 8.48$, representing a shift of 0.12 ppm to higher field, and $\delta_{C^\alpha H} = 3.92$, a shift of 0.01 ppm

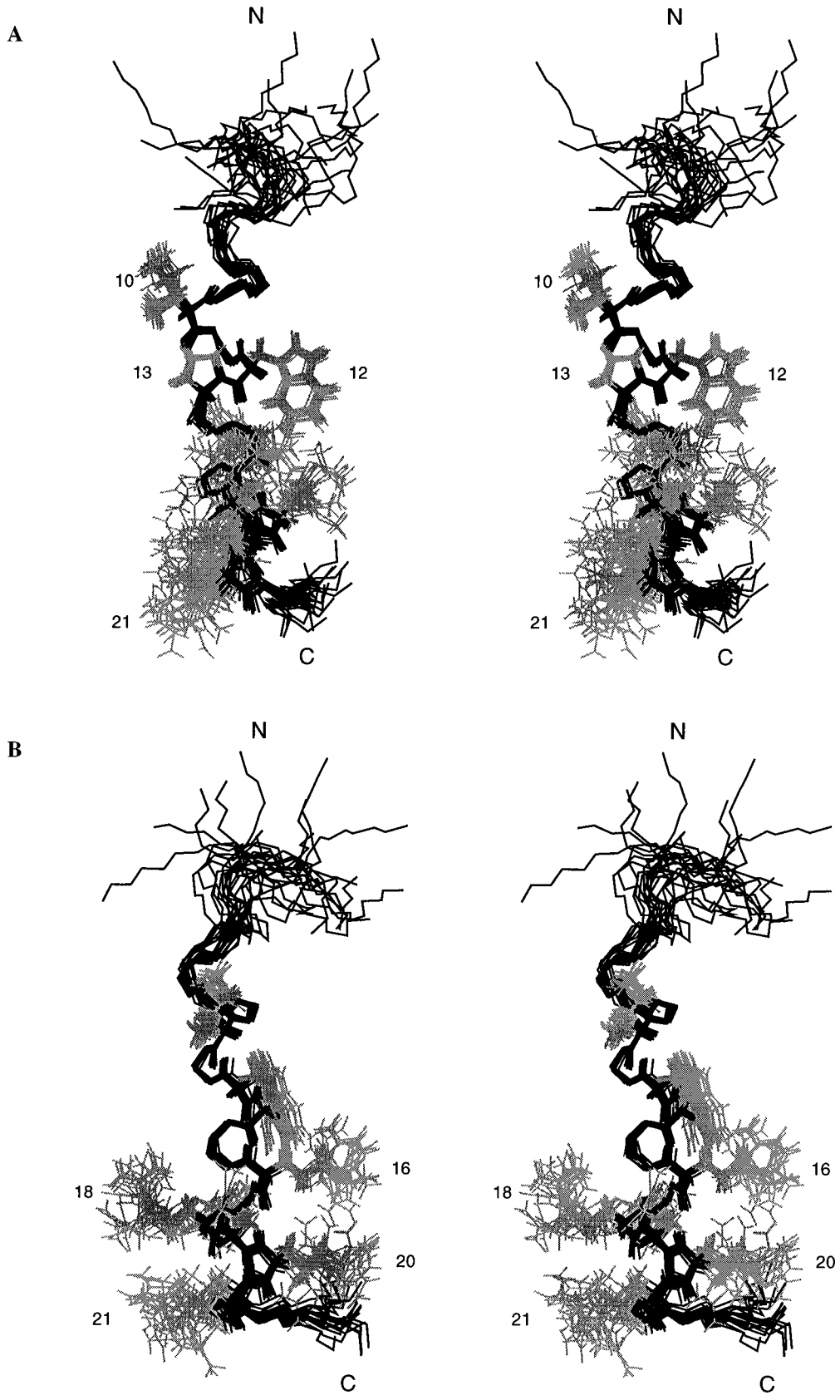

FIGURE 6: Stereoviews of the final 20 structures of Nef1−25 in methanol superimposed over the backbone heavy atoms (N, C^{α}, and C) of the well-defined (S_{ϕ} and S_{ψ} > 0.9) region of the molecule, encompassing residues 7−23. Backbone heavy atoms (bold) and side chains of residues with well-defined χ^1 angles (S_{χ^1} > 0.9) are shown. The two views are related by a 90° rotation about the vertical axis.

to lower field). Otherwise, the spectra were essentially identical. The same medium-range NOESY cross-peaks were also observed. It appeared, therefore, that the myristyl group had no effect on the α-helical structure in methanol.

When the N-terminal acetyl group was replaced by NH_3^+ and the C-terminal amide by a carboxylate, several changes were observed in the spectra, mostly from protons near the N terminus. The NH−C^{α}H cross-peaks for residues 1−7

were quite weak compared with those for other residues, and the NH signals were quite broad (≥18 Hz) in the 1D spectrum, suggesting that some intermediate exchange process was occurring. Consistent with this, the line widths of resolved amide resonances from this region decreased as the temperature was raised to 298 K. The amide chemical shifts of these residues also moved to lower field, by 0.03 (Ser5) to 0.14 ppm (Lys3), presumably due to the effect of the positive charge at the N terminus. The effect on the $C^{\alpha}H$ shifts was smaller (0.03−0.05 ppm) and not consistently in one direction. The effect of deamidation at the C terminus was even less significant, with only the NH peak of Ala25 shifting significantly, to lower field by 0.18 ppm. Other residues were largely unaffected by the changes at the N and C termini. The NOESY spectrum showed that the $d_{\alpha N}(i,i+3)$, $d_{\alpha N}(i,i+4)$, and $d_{\alpha\beta}(i,i+3)$ NOEs characteristic of the α-helix were preserved (compared with the NOESY spectrum of Nef1−25 in methanol), suggesting that the α-helical region of the structure in methanol was essentially unaffected by changes at the N and C termini.

Spectra of Nef1−25 with free N and C termini in water at pH 4.5 and 281 K were very similar to those of Nef1−25. When the *N*-acetyl group was replaced by a myristyl group, however, spectra recorded in water at pH 4.5 showed broad lines (for example, the width at half-height of the indole NH of Trp4 was 5 Hz for Nef1−25 but 15 Hz for myr-Nef1−25), and the 2D NOESY and TOCSY spectra showed very few clear cross-peaks. Thus, it appeared that myristylated Nef1−25 was aggregating in aqueous solution.

DISCUSSION

The NMR data presented in this paper provide clear experimental evidence that the N-terminal amino acid sequence of the Nef protein is capable of adopting an α-helical structure. In dilute aqueous solution, the N terminus is unstructured, but in nonpolar, membrane-like environments, this helical structure is quite stable. In this section, the helical structure is described in more detail and compared with that of melittin in a similar environment, and then the possible biological implications of the structure are discussed.

The chemical shift index plot (Wishart et al., 1991) for Nef1−25 in methanol implied that there were two helices, from residues 3 to 9 and 13 to 21. By contrast, although the $^3J_{NHC^{\alpha}H}$ coupling constants supported the presence of the second helix, with these residues having values consistently below 6 Hz, they were ambiguous with respect to the first, with $^3J_{NHC^{\alpha}H}$ being less than 6 Hz for Lys3 and Lys6 but in the range of 6−8 Hz for other residues in this region. The pattern of medium-range NOE cross-peaks [$d_{\alpha N}(i,i+3)$, $d_{\alpha N}(i,i+4)$, and $d_{\alpha\beta}(i,i+3)$] and the location of medium and slowly exchanging amide protons were consistent with a stable helical structure encompassing residues 6−22, preceded by a less stable, helical-like structure, resembling a nascent helix (Dyson et al., 1988), encompassing residues 3−5. The observation that the amide exchange rates of Trp4 and Ser5 were slower than those of flanking residues (although still fast compared with those of residues 9−23) is consistent with this description.

Proline residues are known to destabilize helices, usually causing bends or kinks, on average by ∼20° (Barlow & Thornton, 1988). The helix of Nef1−25 appears to have a similar kink at Pro13. The amide exchange rates around Pro13 were faster than elsewhere in the helix (Figure 4), suggesting that the absence of a hydrogen bond between Val9 CO and Pro13 may allow some flexibility around Ile10, Gly11, and Trp12. Similar behavior was observed for the amides of the residues flanking Pro14 in melittin (Bazzo et al., 1988). The CSI plot (Figure 4) indicates that the helix is perturbed in this region, and the final family of structures (Figure 6) shows a kinked helical structure, although the location of the kink is not clear from inspection of the ϕ and ψ angles of the angular average over the family. Glu23 is not part of the helix even though its amide exchange rate is intermediate; it has a $^3J_{NHC^{\alpha}H}$ of 8.2 Hz and a low-field shifted $C^{\alpha}H$, both consistent with an extended structure.

The structure of Nef1−25 in methanol is very similar to that of melittin in the same solvent (Bazzo et al., 1988) and in a tetramer crystallized from aqueous solution (Terwilliger & Eisenberg, 1982; Terwilliger et al., 1982), as shown in Figure 7. The C-terminal regions of the helices superimpose very well, but the kink at the proline is not as pronounced in Nef1−25 as in melittin. It should be noted, however, that the solution structure of melittin also has a less pronounced kink than in the crystal structure, so this difference may not be significant. Nevertheless, there is a real difference between the two structures in the N-terminal region, where Nef1−25 is less structured than melittin. As summarized in Figures 4 and 6, there is little evidence for a stable helical structure at the N terminus of Nef1−25, whereas in melittin, the NMR data (backbone coupling constants and medium-range NOEs) were consistent with helices involving residues 2−11 and 13−24, the discontinuity being due to the proline.

The similarities in sequence and structure between melittin and Nef1−25 suggest that they may interact with membranes in a similar fashion. The results of structural and functional studies on melittin have led to two models for its mode of action (Bernheimer & Rudy, 1986). The first has melittin creating aqueous channels by spanning the membrane and forming channel oligomers, exposing its hydrophobic face to the lipid and its hydrophilic face to the aqueous pore. It is predicted that these channels will lead to an ionic imbalance which will produce colloid osmotic lysis. The second model proposes that melittin causes lysis by disrupting the phospholipid structure of the membrane, and several methods by which melittin could achieve this have been suggested. Melittin-like peptides of ≥20 residues (presumably long enough to span a bilayer membrane) and having at least some positively charged residues all appear to have some membrane-perturbing ability (Dawson et al., 1978; Werkmeister et al., 1993; Rivett et al., 1996). Hydrophobic residues are also important. The omission of individual leucine residues in the middle of the hydrophobic face, or of Trp19, led to significant increases (2 orders of magnitude) in the HD_{50} (concentration of peptide required to cause 50% hemolysis), while omission of residues toward the edge of the hydrophobic face (e.g. Ile2, Val5, and Ile20) caused an order of magnitude increase (Blondelle & Houghton, 1991). The omission of individual positively charged residues from the C terminus had a negligible effect on hemolytic activity. In this study, Lys7 also appeared to be important, its deletion being associated with a 30-fold increase in HD_{50}. More recent work, however, indicated that it could be replaced by Ser (Werkmeister et al., 1993) or Trp (Blondelle et al., 1993) without any significant effect on cytolytic activity.

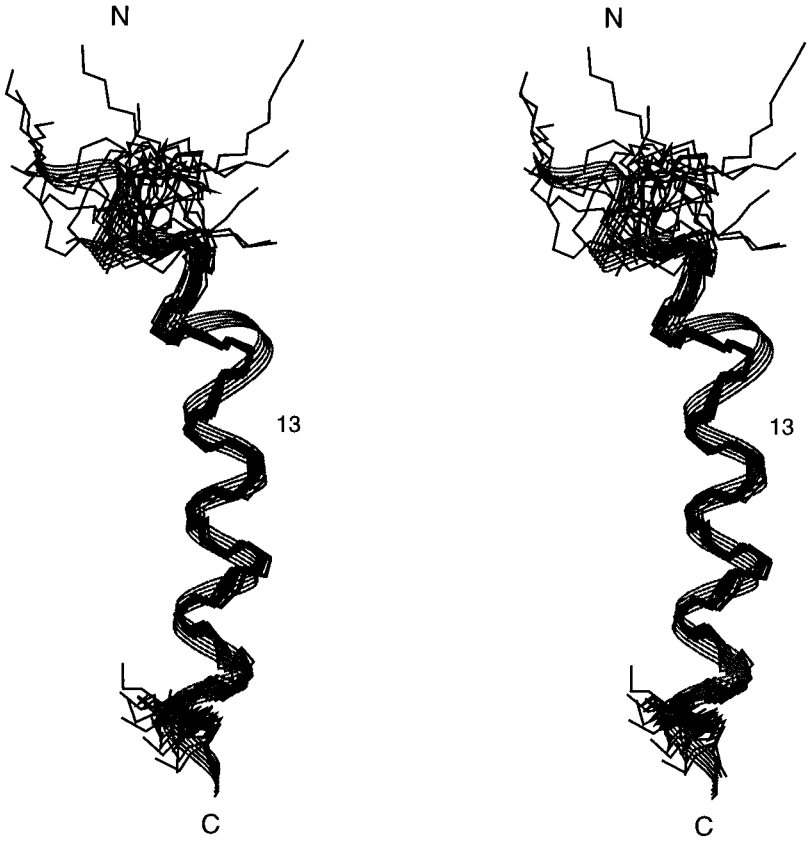

FIGURE 7: Final family of 20 structures of Nef1−25 in methanol [superimposed over the backbone heavy atoms (N, C^{α}, and C) of the well-defined (S_{ϕ} and S_{ψ} > 0.9) region of the molecule, encompassing residues 7−22] overlayed with the crystal structure of melittin (Terwilliger & Eisenberg, 1982) (residues 8−23) (PDB accession code 2MLT). The C-terminal helix of melittin superimposes very well with the Nef1−25 helix, but the large kink (~60°) which is present in the melittin crystal structure is not as pronounced in Nef1−25. Note that the kink in the NMR structure (Bazzo et al., 1988) of melittin is also less pronounced, at 20°.

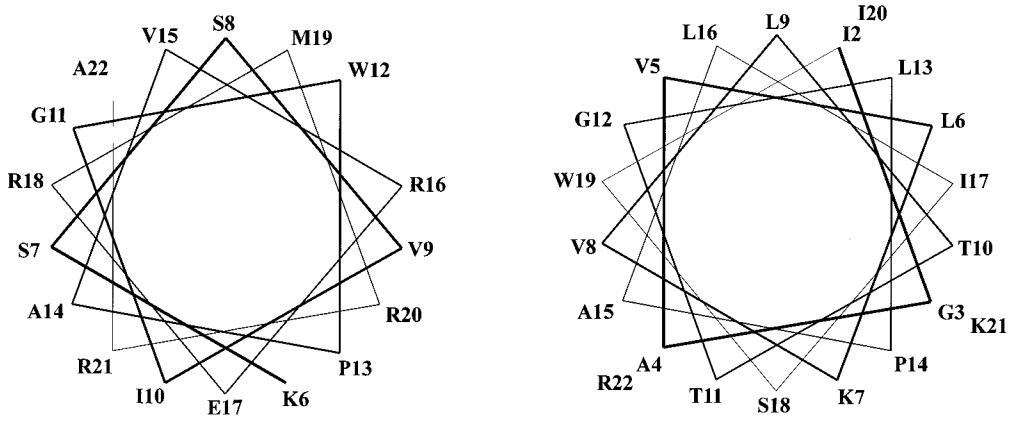

FIGURE 8: (A) α-Helical region of Nef1−25 in methanol (residues 6−22) viewed as an axial projection in a helical wheel presentation, demonstrating the amphipathic nature of the peptide. The small hydrophobic face of the helix is defined by the arc encompassing residues W12 and A22. The rest of the wheel is characterized by well-dispersed hydrophilic residues. (B) Similar view of the α-helical region of melittin (residues 2−22). In comparison with Nef1−25, the hydrophobic face (the arc encompassing residues V5 and I17) is much larger.

The Nef1−25 peptide has a smaller hydrophobic face and a larger hydrophilic face than melittin, as shown by the helical wheel diagrams in Figure 8. This might be expected to make it less effective as a membrane-perturbing agent than melittin. The Nef1−25 peptide also has a marked concentration of charged residues at the C-terminal end of the molecule, with two glutamate and four arginine residues between residues 16 and 23. Melittin has a cluster of four positively charged residues near the C terminus, two of which align with those in Nef1−25. These positively charged residues have been implicated in the action of melittin, although it appears to be the presence of one or more such residues rather than their exact position that is important (Blondelle & Houghton, 1991; Werkmeister et al., 1993). Thus, the ability to form an amphipathic helix and the presence of positive charges are both important to the lytic activity of melittin. Recently, it has been shown that myristylated N-terminal peptides of Nef cause rapid lysis of

a number of cell types (Curtain et al., 1997; Macreadie et al., 1997). The nonmyristylated form was less potent as a lytic agent, but still had measurable activity.

A high-resolution structure for the Nef1−25 peptide in SDS micelles has not been determined in this paper, but it is clear from the NMR data for this system that helical structure is present in the C-terminal part of the molecule, consistent with the structure in methanol. It appears, however, that the N-terminal region is more structured (although not helical) in the micelles than in other solvents, possibly due to interactions of the lysine residues at positions 3 and 6 with the negatively charged detergent head groups. Similar interactions might also be possible with negatively charged lipid head groups in biological membranes.

In aqueous solution, no stable structure was observed for the Nef1−25 peptide, in keeping with the observation by Freund et al. (1994) that residues 2−65 in the intact protein were largely unstructured in aqueous solution. In dilute aqueous solution (<1 mM), melittin also had no regular structure, but at higher concentrations and a variety of pH values and salt concentrations, melittin aggregated and the helical content of the molecule increased (Bello et al., 1982; Quay & Condie, 1983; Maurer et al., 1991). One set of conditions which induced tetramer formation in melittin was 150−200 mM aqueous phosphate buffer. In the case of Nef1−25, addition of up to 300 mM phosphate buffer at pH 5.3 produced no change in the 1D spectrum. We have not investigated the effects of high concentrations on the Nef peptide, but it seems that it is less prone to aggregation than melittin, presumably a reflection of its smaller hydrophobic surface.

Myristylation has been shown to be vitally important to the functions of Nef (Zazopoulos & Haseltine, 1992), but myristylation of Nef1−25 did not significantly affect the structure of the molecule in methanolic solution, when compared with either the acetyl or free ammonium forms of the peptide. Myristylation is probably important primarily for membrane targeting and anchoring of the Nef peptide or protein to the membrane and may have no further role in the interaction of the N-terminal region with the membrane. Indeed, it is possible that the flexible residues near the N terminus assist in allowing the succeeding Nef residues to interact with the membrane in a manner similar to that of melittin, even though the myristyl group is still associated with the membrane. This hypothesis can be tested using synthetic analogues with key substitutions in this region. It should be recalled that residues 2−7 were found to be highly conserved in 54 Nef genes isolated from 12 patients (Shugars et al., 1993), and Goldsmith et al. (1995) showed that residues 4−7 were important for Nef infectivity.

In conclusion, Nef is a multifunctional protein, and it has been shown that the N terminus is of vital importance to some of these functions. In aqueous solution, the N terminus is unstructured, but it is likely that the functions of this region of the protein involve interactions with cell membranes, in which environment the structure is probably significantly different from that in aqueous solution. The structure of Nef1−25 in methanol, as described in this paper, may be expected to resemble more closely the structure adopted by the N terminus of Nef when it interacts with cell membranes. We are now investigating the structures and membrane-perturbing activities of further analogues of the N-terminal region to establish the functional significance of both the helical and flexible regions of the sequence.

ACKNOWLEDGMENT

We thank Paul Pallaghy for assistance and advice, Don Rivett and Cyril Curtain for helpful discussions, John MacFarlane and Marilyn Olliff for assistance with computing, Till Maurer for recording preliminary spectra, David Craik for the provision of the program COUPLING, and Alan Kirkpatrick for peptide synthesis.

SUPPORTING INFORMATION AVAILABLE

Table of ^{1}H NMR chemical shifts and assignments for Nef1−25 in methanol at pH 4.5 and 281 K (1 page). Ordering information is given on any current masthead page.

REFERENCES

Allan, J. S., Coligan, J. E., Lee, T.-H., McLane, M. F., Kanki, P., Groopman, J. E., & Essex, M. (1985) *Science 230*, 810−813.

Anil-Kumar, Ernst, R. R., & Wüthrich, K. (1980) *Biochem. Biophys. Res. Commun. 95*, 1−6.

Artenstein, A. W., Hiegerich, P. A., Beyrer, C., Rungruengthanakit, K., Michael, N. L., & Natpratan, C. (1996) *AIDS Res. Hum. Retroviruses 12*, 557−560.

Barlow, D. J., & Thornton, J. M. (1988) *J. Mol. Biol. 201*, 601−619.

Bartels, C., Xia, T.-H., Billeter, M., Güntert, P., & Wüthrich, K. (1995) *J. Biomol. NMR 5*, 1−10.

Bax, A., Griffey, R. H., & Hawkins, B. L. (1983) *J. Magn. Reson. 55*, 301−315.

Bazzo, R., Tappin, M. J., Pastore, A., Harvey, T. S., Carver, J. A., & Campbell, I. D. (1988) *Eur. J. Biochem. 173*, 139−146.

Bello, J., Bello, H. R., & Grandos, E. (1982) *Biochemistry 21*, 461−465.

Bernstein, F. C., Koetzle, T. F., Williams, G. J. B., Meyer, E. F., Brice, M. D., Rodgers, J. R., Kennard, O., Shimanouchi, T., & Tasumi, M. (1997) *J. Mol. Biol. 112*, 535−542.

Blondelle, S. E., & Houghten, S. E. (1991) *Biochemistry 30*, 4671−4678.

Blondelle, S. E., Simpkins, L. R., Perez-Paya, E., & Houghten, S. E. (1993) *Biochim. Biophys. Acta 1202*, 331−336.

Braunschweiler, L., & Ernst, R. R. (1983) *J. Magn. Reson. 53*, 521−528.

Brooks, B. R., Bruccoleri, R. E., Olafson, B. D., States, D. J., Swaminathan, S., & Karplus, M. (1983*) J. Comput. Chem. 4*, 187−217.

Brown, L. R., & Wüthrich, K. (1981) *Biochim. Biophys. Acta 647*, 95−111.

Brown, L. R., Braun, W., Anil-Kumar, & Wüthrich, K. (1982) *Biophys. J. 37*, 319−328.

Brünger, A. T. (1992) *X-PLOR Version 3.1. A system for X-ray Crystallography and NMR*, Yale University, New Haven, CT.

Cullen, B. R. (1994) *Virology 205*, 1−6.

Curtain, C. C., Separovic, F., Rivett, D., Kirkpatrick, A., Waring, A. J., Gordon, L. M., & Azad, A. A. (1994) *AIDS Res. Hum. Retroviruses 10*, 1231−1239.

Curtain, C. C., Lowe, M. G., Arunagiri, C. K., Mobley, P. W., Macreadie, I. G., & Azad, A. A. (1997) *AIDS Res. Hum. Retroviruses* (in press).

Dawson, C. R., Drake, A. F., Helliwell, J., & Hider, R. C. (1978) *Biochim. Biophys. Acta 510*, 75−86.

Deacon, N. J., Tsykin, A., Solomon, A., Smith, K., Ludford-Menting, M., Hooker, D. J., McPhee, D. A., Greenway, A. L., Ellet, A., Chatfield, C., Lawson, V. A., Crowe, S., Maerz, A., Sonza, S., Learmont, J., Sullivan, J. S., Cunningham, A., Dwyer, D., Dowton, D., & Mills, J. (1995) *Science 270*, 988−991.

Dyson, H. J., Rance, M., Houghten, R. A., Wright, P. E., & Lerner, R. A. (1988) *J. Mol. Biol. 201*, 201−217.

Dyson, H. J., Merutka, G., Waltho, J. P., Lerner, R. A., & Wright, P. E. (1992) *J. Mol. Biol. 226*, 795−817.

Freund, J., Kellner, R., Houthaeve, T., & Kalbitzer, H. R. (1994) *Eur. J. Biochem. 221*, 811−819.
Goldsmith, M. A., Warmerdam, M. T., Atchison, R. E., Millar, M. D., & Greene, W. C. (1995) *J. Virol. 69*, 4112−4121.
Greenway, A. L., McPhee, D. A., Grgacic, E., Hewish, D., Lucantoni, A., Macreadie, I., & Azad, A. (1994) *Virology 198*, 245−256.
Greenway, A. L., Azad, A., & McPhee, D. A. (1995) *J. Virol. 69*, 1842−1850.
Griesinger, C., Sørenson, O., & Ernst, R. R. (1987) *J. Magn. Reson. 75*, 474−492.
Grzesiek, S., Bax, A., Clore, G. M., Gronenborn, A. M., Hu, J.-S., Kaufman, J., Palmer, I., Stahl, S. J., & Wingfield, P. T. (1996) *Nat. Struct. Biol. 3*, 340−345.
Güntert, P., Braun, W., & Wüthrich, K. (1991) *J. Mol. Biol. 217*, 517−530.
Guy, B., Kieny, M. P., Riviere, Y., LePeuch, C., Girard, M., Montagnier, L., & Lecocq, J. P. (1987) *Nature 330*, 266−269.
Hyberts, S. G., Goldberg, M. S., Havel, T. F., & Wagner, G. (1992) *Protein Sci. 1*, 736−751.
Ikura, T., Gõ, N., & Inagaki, F. (1991) *Proteins: Struct., Funct., Genet. 9*, 81−89.
Inagaki, F., Shimada, I., Kawaguchi, K., Hirano, M., Terasawa, T., & Gõ, N. (1989) *Biochemistry 28*, 5985−5991.
Kaplan, J. M., Mardon, G., Bishop, J. M., & Varmus, H. E. (1988) *Mol. Cell. Biol. 8*, 2435−2441.
Kestler, H. W., III, Ringler, D. J., Mori, K., Panicali, D. L., Sehgal, P. K., Daniel, M. D., & Desrosiers, R. C. (1991) *Cell 65*, 651−662.
Lee, C.-H., Saksela, K., Mirza, U. A., Chait, B. T., & Kuriyan, J. (1996) *Cell 85*, 931−942.
Lee, K. H., Fitton, J. E., & Wüthrich, K. (1987) *Biochim. Biophys. Acta 911*, 144−153.
Ludvigsen, S., & Poulsen, F. M. (1992) *J. Biomol. NMR 2*, 227−233.
Macreadie, I. G., Castelli, L. A., Lucantoni, A., & Azad, A. A. (1995) *Gene 162*, 239−243.
Macreadie, I. G., Lowe, M. G., Curtain, C. C., Hewish, D., & Azad, A. A. (1997) *Biochem. Biophys. Res. Commun.* (in press).
Macura, S., Huang, Y., Suter, D., & Ernst, R. R. (1981) *J. Magn. Reson. 43*, 259−281.
Manoleras, N., & Norton, R. S. (1994) *Biochemistry 33*, 11051−11061.
Marion, D., & Wüthrich, K. (1983) *Biochem. Biophys. Res. Commun. 113*, 967−974.
Maurer, T., Lücke, C., & Rüterjans, H. (1991) *Eur. J. Biochem. 196*, 135−141.
Monks, S. A., Pallaghy, P. K., Scanlon, M. J., & Norton, R. S. (1995) *Structure 3*, 791−803.
Morton, C. J., Simpson, R. J., & Norton, R. S. (1994) *Eur. J. Biochem. 219*, 97−107.
Nelson, J. W., & Kallenbach, N. R. (1986) *Proteins 1*, 211−217.
Pallaghy, P. K., Duggan, B. M., Pennington, M. W., & Norton, R. S. (1993) *J. Mol. Biol. 234*, 405−420.
Piotto, M., Saudek, V., & Sklenar, V. (1992) *J. Biomol. NMR 2*, 661−666.
Quay, S. C., & Condie, C. C. (1983) *Biochemistry 22*, 695−700.
Rance, M., Sørenson, O. W., Bodenhausen, G., Wagner, G., Ernst, R. R., & Wüthrich, K. (1983) *Biochem. Biophys. Res. Commun. 117*, 479−485.
Rivett, D. E., Kirkpatrick, A., Hewish, D. R., Reilly, W., & Werkmeister, J. A. (1996) *Biochem. J. (Part 2) 316*, 525−529.
Rucker, S. P., & Shaka, A. J. (1989) *Mol. Phys. 68*, 509−517.
Sabatier, J.-M., Fontan, G., Loret, E., Mabrouk, K., Rochat, H., Gluckman, J.-C., Montagnier, L., Granier, C., Bahraoui, E., & van Rietschoten, J. (1990) *Int. J. Pept. Protein Res. 35*, 63−72.
Saksela, K., Cheng, G., & Baltimore, D. (1995) *EMBO J. 14*, 484−491.
Schwartz, O., Marechal, V., Danos, O., & Heard, J. M. (1995) *J. Virol. 69*, 4053−4059.
Shugars, D. C., Smith, M. S., Glueck, D. H., Nantermet, P. V., Seillerier-Moiseiwitsch, F., & Swanstrom, R. (1993) *J. Virol. 67*, 4639−4650.
Sönnichsen, F. D., Van Eyk, J. E., Hodges, R. S., & Sykes, B. D. (1992) *Biochemistry 31*, 8790−8798.
Tappin, M. J., Pastore, A., Norton, R. S., Freer, J. H., & Campbell, I. D. (1988) *Biochemistry 27*, 1643−1647.
Terwilliger, T. C., & Eisenberg, D. (1982) *J. Biol. Chem. 257*, 6016−6022.
Terwilliger, T. C., Weissman, L., & Eisenberg, D. (1982) *Biophys. J. 37*, 353−361.
Trono, D. (1995) *Cell 82*, 189−192.
van Geet, A. L. (1970) *Anal. Chem. 42*, 679−680.
Wagner, G., Braun, W., Havel, T. F., Schaumann, T., Gõ, N., & Wüthrich, K. (1987) *J. Mol. Biol. 196*, 611−639.
Werkmeister, J. A., Kirkpatrick, A., McKenzie, J. A., & Rivett, D. E. (1993) *Biochim. Biophys. Acta 1157*, 50−54.
Wilcox, G. R., Fogh, R. H., & Norton, R. S. (1993) *J. Biol. Chem. 268*, 24707−24719.
Wishart, D. S., Sykes, B. D., & Richards, F. M. (1991) *J. Mol. Biol. 222*, 311−333.
Wishart, D. S., Bigam, C. G., Yao, J., Abildgaard, F., Dyson, J., Oldfield, E., Markley, J. L., & Sykes, B. D. (1995a) *J. Biomol. NMR 6*, 135−140.
Wishart, D. S., Bigam, C. G., Holm, A., Hodges, R. S., & Sykes, B. D. (1995b) *J. Biomol. NMR 5*, 67−81.
Wüthrich, K. (1976) *NMR in Biological Research: Peptides and Proteins*, North-Holland, Oxford.
Wüthrich, K. (1986) *NMR of Proteins and Nucleic Acids*, Wiley, New York.
Zazopoulos, E., & Haseltine, W. A. (1992) *Proc. Natl. Acad. Sci. U.S.A. 89*, 6634−6638.
Zhou, N. E., Zhu, B.-Y., Sykes, B. D., & Hodges, R. S. (1992) *J. Am. Chem. Soc. 114*, 4320−4326.

BI9629945